THE JOURNAL OF PHYSICAL CHEMISTRY LETTERS
A JOURNAL OF THE AMERICAN CHEMICAL SOCIETY

pubs.acs.org/JPCL Letter

Why Are Nucleosome Breathing Dynamics Asymmetric?

Anupam Mondal and Anatoly B. Kolomeisky*

Cite This: J. Phys. Chem. Lett. 2024, 15, 422−431 Read Online

ACCESS | Metrics & More | Article Recommendations | Supporting Information

ABSTRACT: In eukaryotic cells, DNA is bound to nucleosomes, but DNA segments occasionally unbind in the process known as nucleosome breathing. Although DNA can unwrap simultaneously from both ends of the nucleosome (symmetric breathing), experiments indicate that DNA prefers to dissociate from only one end (asymmetric breathing). However, the molecular origin of the asymmetry is not understood. We developed a new theoretical approach that gives microscopic explanations of asymmetric breathing. It is based on a stochastic description that leads to a comprehensive evaluation of dynamics by using effective free-energy landscapes. It is shown that asymmetric breathing follows the kinetically preferred pathways. In addition, it is also found that asymmetric breathing leads to a faster target search by transcription factors. Theoretical predictions, supported by computer simulations, agree with experiments. It is proposed that nature utilizes the symmetry of nucleosome breathing to achieve a better dynamic accessibility of chromatin for more efficient genetic regulation.

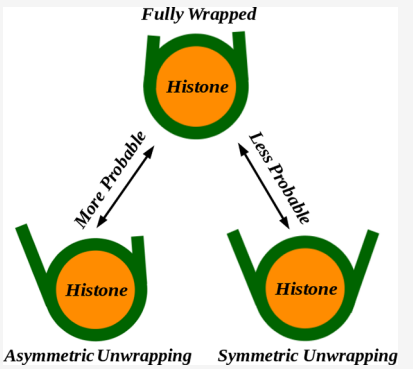

DNA molecules are long biological polymers that contain all genetic information about living organisms, and in order to fit into small cellular volumes, they are typically bound to nucleosome protein complexes, creating compact chromatin structures.[1,2] However, this presents a problem since all major biological processes, such as transcription, replication, and gene regulation, can start only after specific protein molecules, known as transcription factors (TFs), locate and bind to correct DNA sequences in gene-promoting regions which might be sterically blocked by nucleosomes.[1−4] A single nucleosome is an octamer protein complex that contains two copies of the four histone core proteins, H2A, H2B, H3, and H4, around which ∼150 base pairs (bp) of DNA are tightly wrapped into 1.65 superhelical turns.[5,6] Such tight wrapping of DNA around the histone octamer sterically occludes most TFs from binding to their target sites.[7−9] Experimental studies, however, indicate that chromatin structures are not rigid and DNA might spontaneously unwrap from the nucleosome, transiently exposing the binding sites of many regulatory proteins. This process is known as nucleosome breathing or site exposure.[10−14] It has been shown that at the nucleosome termini, the DNA unwraps and rewraps on millisecond time scales under typical physiological conditions.[12,15] By control of the DNA accessibility within the nucleosome, this rapid partial unfolding of the nucleosomal DNA complexes plays an important role by making chromatin structures more susceptible to efficient genetic regulation.

However, it is important to note that nucleosome breathing does not always result in exposure of the entire DNA length covered by the nucleosome. There are DNA sites that are buried deep inside the nucleosome inner segment, and they remain mostly not accessible. But nature resolves this problem by utilizing a special class of TFs that are known as pioneer TFs. They have the ability to invade the DNA target sites even in inaccessible regions, and subsequently, they create permissive states for the following regulatory processes to occur.[16−21] Therefore, the proper functioning of pioneer TFs is of critical importance because their misregulation can create defects in large-scale chromatin structures and compromise human health.[16] Indeed, pioneer TFs are found both up- and down-regulated, mutated, or amplified in their genomic locus in many forms of cancer.[16,22] The mechanisms by which pioneer TFs can access the nucleosome-covered DNA remain not well understood,[23−25] although several theoretical ideas to explain their functioning have been already proposed.[23,26−30]

Dynamics of wrapping/unwrapping of DNA from individual nucleosomes has been intensively investigated in recent times using a variety of experimental techniques.[11−13,31−37] These studies revealed that, surprisingly, despite the ability to dissociate from both ends of the nucleosome, DNA strongly prefers to unwrap from only one end. For example, time-resolved small-angle X-ray scattering measurements of nucleosome disassembly revealed the asymmetric release of DNA from the histone core for different DNA sequences.[36,38] Similarly, asymmetric unwrapping of nucleosomal DNA has been observed using time-resolved FRET measurements.[37] Several arguments to explain this asymmetry have been

Received: November 28, 2023
Revised: December 28, 2023
Accepted: January 3, 2024

https://doi.org/10.1021/acs.jpclett.3c03339
J. Phys. Chem. Lett. 2024, 15, 422−431

proposed. It was suggested that it might be associated with the sequence-dependent mechanical properties of DNA chains.[35,38] But it seems that asymmetric nucleosome breathing occurs in DNA with very different sequences.[36] From the studies based on cryo-EM and atomic force microscopy, it was also proposed that the one-sided unwrapping is favored more because the partial unwrapping of one nucleosomal end helps to stabilize the other end.[39−41] However, the nature of conformational changes in nucleosomes that lead to this effect is not fully understood. Furthermore, molecular dynamics simulations have been recently actively used to quantify the free-energy landscapes of nucleosome breathing, and these computational studies again indicated that the unwrapping should proceed mostly along an asymmetric path.[14,42−44] Thus, despite several proposed ideas, a clear molecular picture of why nucleosome breathing prefers to be asymmetric has not yet emerged.

To understand the molecular origin of asymmetry in nucleosome breathing, in this Letter we develop a novel theoretical method for investigating these processes. It is based on mapping DNA wrapping and unwrapping from the nucleosome into a network of stochastic transitions between individual states that allows us to analyze the underlying processes via an effective free-energy landscape. Using this theoretical approach, we explicitly evaluate the dynamic properties of nucleosome breathing by utilizing a method of first-passage probabilities. It is found that free-energy pathways that correspond to asymmetric breathing are much more probable than those that correspond to symmetric breathing. In addition, our theoretical calculations suggest that asymmetric nucleosome breathing accelerates the search for hidden DNA sites by pioneering TFs as compared with symmetric nucleosome breathing. The estimated search times fully agree with the available experimental observations, and analytical calculations are also fully supported by Monte Carlo computer simulations. Based on these results, we suggest that nature selected asymmetric nucleosome breathing as an efficient approach to make chromatin structures more accessible for the activation of gene regulation processes.

The dissociation of DNA from the nucleosome particle can occur via different scenarios, as schematically shown in Figure 1. During asymmetric breathing, DNA unwraps from one end only, while both DNA ends detach in symmetric breathing. To understand the role of symmetry in nucleosome breathing, we first analyze a process of eviction of the whole nucleosome from DNA. However, one should also mention that the same arguments can be applied for more probable partial nucleosome disassembly events. The idea is to look for all possible unwrapping and wrapping pathways in terms of an effective free-energy landscape created by transitions between structurally distinct states of the system. Then considering only two limiting pathways as representatives of the overall trends for nucleosome breathing being symmetric or asymmetric, the probabilities of different outcomes are explicitly evaluated.

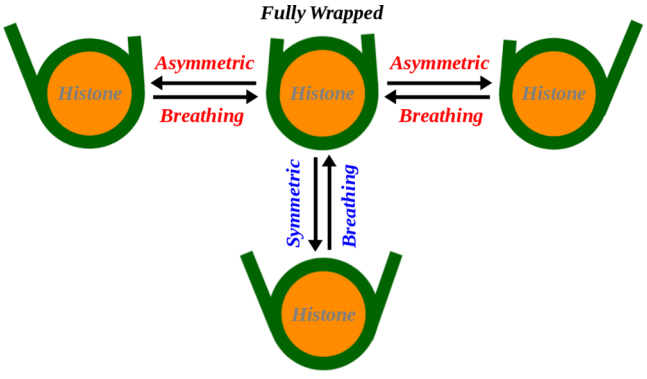

Figure 1. Schematic representation of the asymmetric and symmetric nucleosome breathing processes. In asymmetric breathing, a segment of DNA can partially unwrap from only one end, whereas both DNA ends can dissociate in symmetric nucleosome breathing. The nucleosomal DNA is shown as a green solid line, and the histone protein is represented by an orange circle.

Now let us consider a nucleosome eviction process. It is assumed that the process always starts from the fully bound DNA-nucleosome complex in which ∼150 bps of DNA are wrapped around the histone protein. The DNA molecule is viewed as a lattice of $L = 15$ sites, and each site is equivalent to about 10 bps, which corresponds to a typical size of target sequences for TFs.[3,45] At any moment, the system can be found in one of the discrete states that are specified by how much DNA is already liberated from the nucleosome (Figure 2). There are in total $\frac{17 \times 16}{2} = 136$ states that are labeled as (n_1, n_2) with $0 \le n_1 + n_2 \le 15$, and n_1 and n_2 are the numbers of DNA sites dissociated from the left and right ends of the DNA-nucleosome complex, respectively (see Supporting Information Figure S1). Only one DNA site is allowed to be dissociated from the histone or reassociated with the nucleosome for each event. The transition rate to unwrap one DNA site is assumed to be equal to u, while the reverse wrapping transition rate is w. The number of DNA sites in each state that are still covered by the nucleosome is equal to $15 - n_1 - n_2$. It is also assumed that the unwrapping and wrapping rates in our system are independent of the DNA sequence and of the number of bound DNA sites (Figure 2).

It can be argued that the wrapping and unwrapping transition rates are related to the free-energy cost ΔG of breaking the bond between the nucleosome and a single DNA site. Using the detailed balance-like arguments,[46,47] it can be shown that

$$\frac{u}{w} = e^{-\Delta G/k_B T} \tag{1}$$

where k_B is Boltzmann's constant and T is the temperature. This allows us to obtain explicit expressions for association/dissociation rates,

$$u = k_0 e^{-\theta \Delta G/k_B T}, \; w = k_0 e^{(1-\theta)\Delta G/k_B T} \tag{2}$$

where k_0 is an attempt rate for unwrapping and wrapping processes for the situation when there is no associated free-energy change. The parameter $0 \le \theta \le 1$ specifies how much of the free energy associated with the DNA−nucleosome bond breaking is distributed between the wrapping and unwrapping processes.[48] In our calculations, we assume $\theta = 0.5$, but it can be shown that specific values of θ do not affect our predictions.

Our theoretical approach maps nucleosome breathing processes into a set of stochastic transitions between different chemical states, as illustrated in Figure 2. There are multiple pathways between the fully wrapped state $(0, 0)$ and the state when the nucleosome is fully evicted $(k, 15 - k)$ with $0 \le k \le 15$. However, to understand the role of symmetry, we concentrate on two limiting pathways (see Figure 2). The horizontal pathway $(0, 0) \rightarrow (15, 0)$ and the vertical pathway

https://doi.org/10.1021/acs.jpclett.3c03339
J. Phys. Chem. Lett. 2024, 15, 422−431

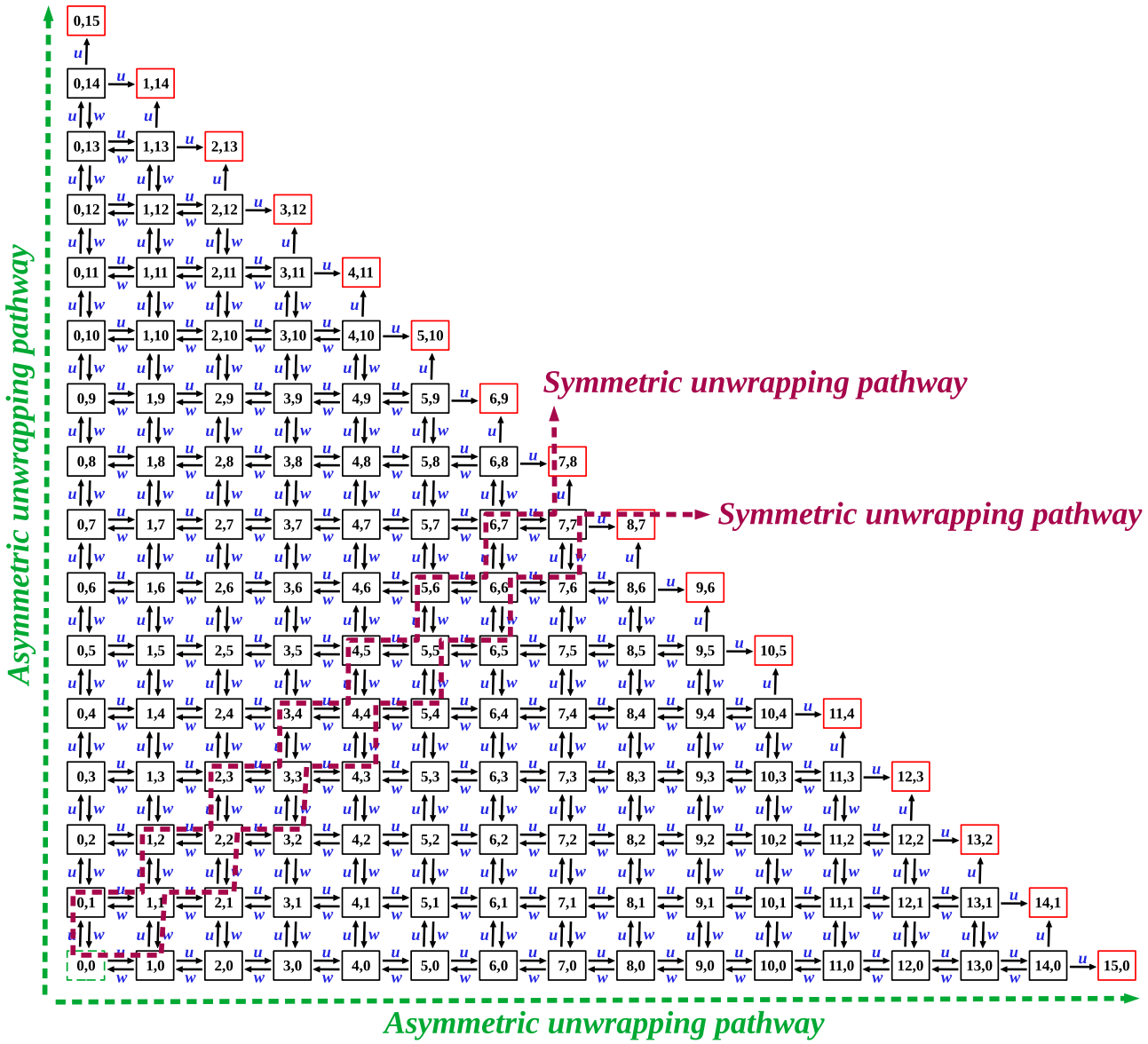

Figure 2. Discrete-state stochastic model of nucleosome eviction. DNA wrapping/unwrapping processes are viewed as stochastic transitions between states (n_1, n_2). The eviction process always starts from the fully wrapped state (0, 0), indicated by the green dashed box. At each time, only one DNA site can dissociate and/or associate from the nucleosome, and the corresponding transition rates are denoted by u and w. The states indicated by red boxes correspond to the fully evicted nucleosome. Green dashed lines describe asymmetric pathways, while magenta dashed lines describe symmetric pathways.

(0, 0) → (0, 15) both correspond to purely asymmetric nucleosome breathing when DNA dissociates always only from one end: see the green dashed lines in Figure 2. At the same time, diagonal pathways (0, 0) → (7, 8) and (0, 0) → (8, 7) describe purely symmetric breathing when DNA alternates between dissociating segments from both ends of the nucleosome (magenta dashed lines in Figure 2). Our goal is to fully characterize and compare the dynamics of nucleosome eviction along one strictly symmetric and one strictly asymmetric pathway because they reflect different modes of nucleosome breathing. The idea here is that those two pathways correctly represent all other paths in the specific direction of nucleosome breathing. Then comparing the probabilities of going along these two limiting paths would give us the overall preferences for nucleosome breathing.

To obtain a dynamic description of nucleosome breathing, we utilize a method of first-passage probabilities that has been widely used for investigations of complex chemical and biological processes.[48,49] One can introduce a probability density function $F^{Asym}_{(n_1,n_2=0)}(t) = F^{Asym}_{n_1}(t)$, which is defined as the probability to reach for the first time the fully unwrapped state (15, 0) at time t by moving only along the asymmetric horizontal pathway if initially (at $t = 0$) the system started at the state $(n_1, n_2 = 0)$: see Figure 2 and Supporting Information Figure S2. The temporal evolution of these functions can be described by a set of backward master equations,[49]

$$\frac{dF^{Asym}_{n_1}(t)}{dt} = uF^{Asym}_{n_1+1}(t) + wF^{Asym}_{n_1-1}(t) - (2u + w)F^{Asym}_{n_1}(t) \tag{3}$$

for $0 < n_1 < 15$, while for $n_1 = 0$ we have

https://doi.org/10.1021/acs.jpclett.3c03339
J. Phys. Chem. Lett. 2024, 15, 422−431

$$\frac{dF_0^{Asym}(t)}{dt} = uF_1^{Asym}(t) - 2uF_0^{Asym}(t) \tag{4}$$

In addition, we have the condition $F_{n_1=15}(t) = \delta(t)$, which means that if the system starts already in the fully unwrapped state then the process of nucleosome eviction is immediately accomplished.

As shown in detail in the Supporting Information, eqs 3 and 4 can be analytically solved by using Laplace transformations $\left(\widetilde{F_{n_1}^{Asym}}(s) = \int_0^\infty e^{-st}F_{n_1}^{Asym}(t)dt\right)$, providing a comprehensive description of the dynamics of nucleosome breathing along the asymmetric pathway at all times. More specifically, it allows us to evaluate the probability that the system follows this asymmetric pathway that can be associated with the corresponding splitting probability,

$$\Pi_{Asym} = \int_0^\infty F_{n_1}^{Asym}(t)dt = \widetilde{F_{n_1}^{Asym}}(s=0) \tag{5}$$

In addition, the mean first-passage time (MFPT) to reach the fully unwrapped state through the asymmetric pathway can be also evaluated,

$$T_{evic}^{Asym} = \frac{1}{\Pi_{Asym}}\int_0^\infty tF_{n_1}^{Asym}(t)dt = \frac{-\frac{\partial\widetilde{F_{n_1}^{Asym}}(s)}{\partial s}|_{s=0}}{\Pi_{Asym}} \tag{6}$$

A similar analysis can be done for the symmetric pathway, and the details of corresponding calculations are given in the Supporting Information.

Now, we can explicitly evaluate the probabilities of symmetric and asymmetric routes for full nucleosome eviction. This can be done by calculating the probabilities for each route. It is convenient to define a ratio of such probabilities,

$$R_\Pi = \frac{\Pi_{Asym}}{\Pi_{Sym}} \tag{7}$$

since it quantifies how the asymmetric pathway is more probable than the symmetric pathway.

The results of our calculations of the parameter R_Π as a function of the free-energy cost of dissociating a single DNA site from the nucleosome are presented in Figure 3. One can see that the asymmetric nucleosome breathing pathways are 2−4 orders of magnitude more probable than the symmetric nucleosome breathing pathways for ΔG ranging between 0 and 5 k_BT. There are experimental measurements of the free-energy cost of unwrapping DNA segments,[50] and for detaching 10 bps of DNA, which corresponds to dissociating 1 site in our discrete-state stochastic model, it can be estimated that $\Delta G \approx 0.3\ k_BT$. This experimental value is shown as a black circle in Figure 3. Even for this relatively weak free-energy cost, our theoretical approach predicts that the asymmetric pathway will be ∼300 times more probable than the symmetric pathway. It is also important to add that mean nucleosome eviction times along each path, as calculated explicitly in the Supporting Information (Figure S3), are similar for both routes (∼5−7 s for the experimental ΔG), and they also agree with experimental estimates.[37] Furthermore, although the probabilities of following each of the two pathways are quite low, the ratio of these probabilities is important since it reflects the preference for the symmetry of nucleosome breathing.

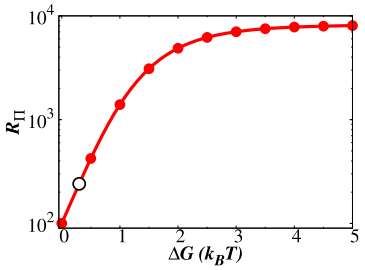

Figure 3. Ratio of splitting probabilities for asymmetric and symmetric nucleosome breathing pathways as a function of the free-energy cost of dissociating a single DNA site from the nucleosome. The solid line is obtained from analytical calculations, and symbols are from Monte Carlo computer simulations. The error bars for each symbol are defined as the standard errors, and the associated error bars are smaller than the symbol size. The black circle highlights the experimentally determined ΔG.[50] The parameters used for the calculation are $k_0 = 1\ s^{-1}$ and $\theta = 0.5$.

In agreement with the experimental observations, our theoretical method predicts that asymmetric nucleosome breathing is the preferred mode of DNA unfolding from the nucleosome. This is because it is the most probable pathway on the route to nucleosome eviction, which also gives time scales similar to those of the symmetric pathway. To explain these observations from a more microscopic point of view, we utilize an effective free-energy landscape picture. Every discrete state (n_1, n_2) in the system (see Figure 2) has a residence time T_{n_1,n_2} that can be determined from the transition rates of leaving this state. Then one can associate the inverse of residence time with an effective free energy of this state,[51]

$$G_{eff}(n_1, n_2) \simeq \ln\left(\frac{1}{T_{n_1,n_2}}\right) \tag{8}$$

This can be explained using the following arguments. The lower the free energy of the given state, the longer the system occupies this state, which is measured by the residence times. The inverse residence time can also be viewed as a rate to escape from the given state. Then assuming that these rates follow the Kramers's-like relation,

$$\frac{1}{T_{n_1,n_2}} \simeq k_{n_1,n_2} \simeq k_0 \exp\left(-\frac{E}{k_BT}\right) \tag{9}$$

where E is the energetic barrier to escape from the given state, it is reasonable to suggest that $\Delta G \approx -E$, leading to eq 8.

Figure 4 presents the effective free-energy landscape for nucleosome breathing processes evaluated by using eq 8. It shows that chemical states located along the horizontal line ($n_2 = 0$) and the vertical line ($n_1 = 0$) have the lowest free energy. This means that the system prefers to move along these asymmetric pathways since they ensure the lowest free energy during nucleosome breathing. All other pathways correspond to higher values of free energy, and for this reason, they are much less visited. The main reason for these observations is the specific values of the residence times. The longest residence time in the system is observed for the state (0, 0), $T_{0,0} = 1/2u$, which corresponds to the fully wrapped state from which the process of DNA unfolding starts. The residence times for horizontal and vertical bound states are shorter, and they are given by $T_{n_1\neq 0,0} = T_{0,n_2\neq 0} = 1/(2u + w)$. For all other states, these times are even shorter, $T_{n_1\neq 0,n_2\neq 0} = 1/(2u + 2w)$.

https://doi.org/10.1021/acs.jpclett.3c03339
J. Phys. Chem. Lett. 2024, 15, 422−431

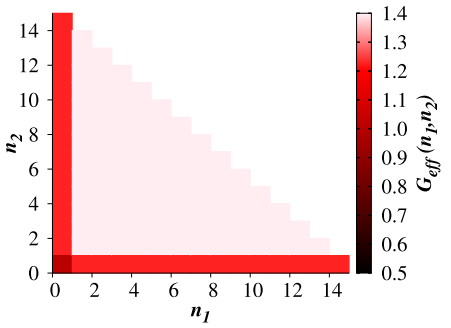

Figure 4. Effective free-energy landscape for the nucleosome eviction process. The parameters used for the calculations are $k_0 = 1\ s^{-1}$, $\theta = 0.5$, and $\Delta G = 0.3k_BT$.

One can see now clearly that the DNA unwrapping process starting in the state (0, 0) with a large probability will proceed only through horizontal states or only through vertical states. These are asymmetric nucleosome breathing pathways. We note here that our theoretical approach suggests that only two asymmetric pathways are special, while all other pathways, including purely symmetric ones, have similar probabilities to be observed.

It is important to note that in nucleosome breathing, the system will follow not only the two limiting pathways that we considered so far. However, it is reasonable to expect that those pathways that lead to the asymmetric outcome more frequently reach the edge states (with $n_1 = 0$ or $n_2 = 0$) than the pathways that lead to the symmetric outcome. Then the asymmetric pathways are more probable from the effective free-energy landscape point of view, supporting our main theoretical conclusion. These arguments probably also explain why the preference for asymmetric nucleosome breathing is universal (sequence-independent). It is also crucial to emphasize that our system is clearly nonequilibrium, and one can see this from the fact that there are nonzero fluxes in the system starting from the initial state and ending in the exit states. We only use the analogy with free energy to better visualize the preferences for the asymmetric pathways in the system. In other words, the fraction of broken contacts is not really a 1D reaction coordinate and strongly depends on which contacts are broken in what particular order. The probability that these contacts will be broken along a specific asymmetric path is different in the sense that these paths are kinetically favored over the symmetric paths. The system unwraps faster via asymmetric pathways, and nucleosome unwrapping is a kinetically controlled process.

Our theoretical analysis so far concentrated only on two limiting pathways, hoping that they correctly represent the overall trends for nucleosome breathing to have symmetric or asymmetric outcomes. But the real system follows multiple pathways (see Figure 2), and it is not obvious that the calculations for the limiting cases correctly describe the nucleosome breathing dynamics at all. To test this, we performed Monte Carlo computer simulations for the system to follow all possible pathways, as explained in detail in the Supporting Information. Specifically, the probabilities of outcomes at different exit states (n_1, n_2) with $n_1 + n_2 = 15$ have been evaluated. Two cases have been analyzed. In the first case, two exit states (7, 8) and (8, 7) are considered symmetric outcomes, and in the second case, we take a more relaxed view of symmetry and define four exit states (6, 9), (7, 8), (8, 7), and (9, 6) as describing symmetric breathing. All other exit states by definition should correspond to asymmetric breathing.

Figure 5 shows the results of computer simulation estimates for the probability of symmetric nucleosome breathing for

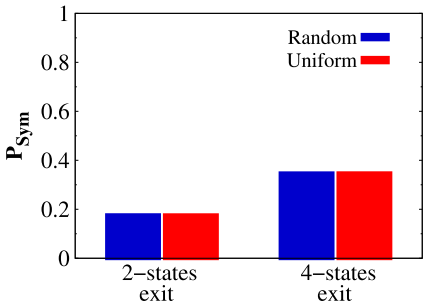

Figure 5. Probability of symmetric unwrapping pathways obtained from Monte Carlo simulations. The red bar corresponds to the situation when a uniform value of $\Delta G = 0.3k_BT$ is considered in the simulation, whereas the blue curve corresponds to the scenario when the value of ΔG in each Monte Carlo simulation is chosen randomly from a Gaussian distribution with mean 0.3 and standard deviation 0.1 to simulate the whole network. The other parameters used for the calculation are $k_0 = 1\ s^{-1}$ and $\theta = 0.5$.

cases with two or four exit states. One can see that taking into account all possible pathways still predicts the symmetric breathing to be less probable: less than 20% for the two exit states case and ∼35% for the case of four exit states. Asymmetric nucleosome breathing ($P_{Asym} = 1 - P_{Sym}$) dominates in all situations.

One of the drawbacks of our theoretical approach is the assumption that all sites on DNA are identical, which is clearly unrealistic, since DNA sequence heterogeneity is an important effect that should be accounted for. To mimic the effect of the DNA sequence, we modify our theoretical model to assume random free energies ΔG to be assigned for transitions in the system. The variations in these free energies would mimic the sequence heterogeneity. Again, it can be analyzed using Monte Carlo simulations, and predictions for the probability of symmetric nucleosome breathing are given in Figure 5. One can see that the random distribution of energies of sites that mimic the DNA sequence effect does not affect our main theoretical predictions. Still, asymmetric nucleosome breathing is more probable. The only effect of the random distribution is that mean search times in the random model become longer in comparison with the uniform situation: see Supporting Information Figure S4.

Having established the preferred mode of nucleosome breathing, it seems reasonable to ask if nature might explore this feature for more efficient access to chromatin. To test this idea, we now investigate the dynamics of the target search for specific sites on DNA for pioneer TFs for symmetric and asymmetric nucleosome breathing processes. Pioneer TFs are special classes of protein molecules that are capable of entering chromatin structures, opening the possibility for other TFs to participate in gene activation processes.[16−21]

We consider a theoretical model for a pioneer TF target search as illustrated in Figure 6. The system contains a single nucleosome particle and a single DNA chain. Since ∼150 bps of DNA are wrapped around the histone core protein in the fully wrapped conformation, we therefore again model the

https://doi.org/10.1021/acs.jpclett.3c03339
J. Phys. Chem. Lett. 2024, 15, 422−431

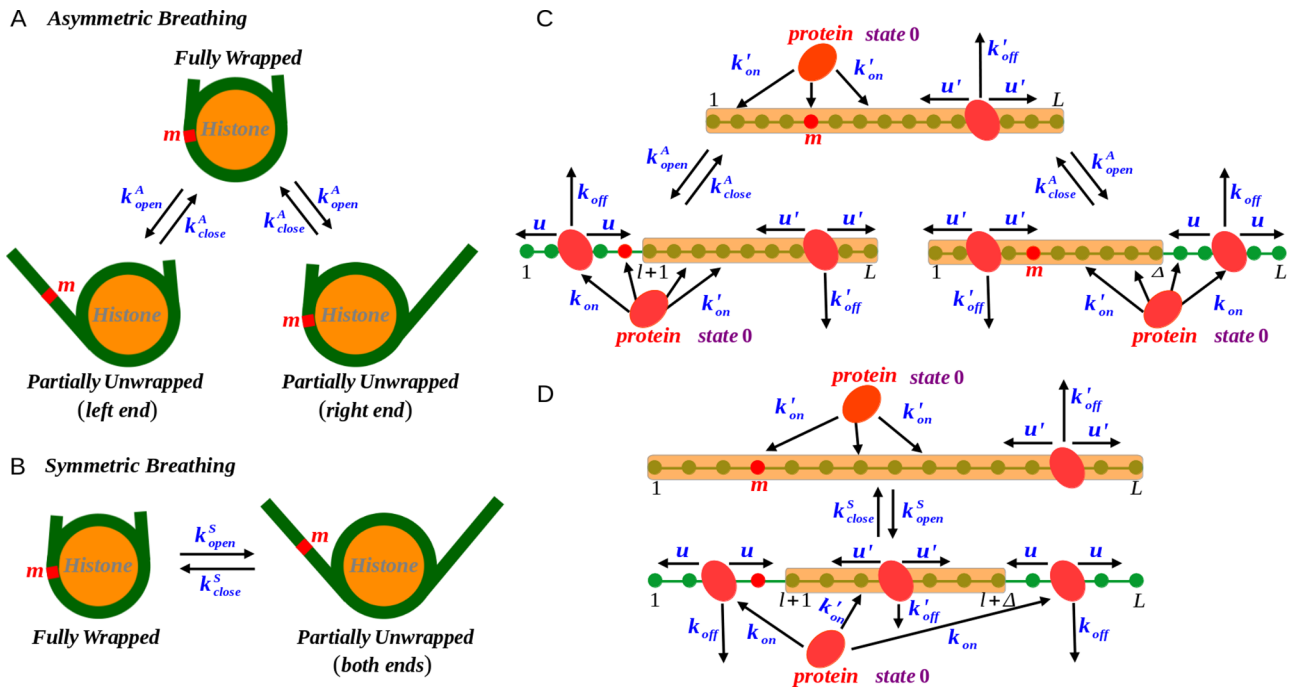

Figure 6. Schematic view of conformational transitions in (A) asymmetric nucleosome breathing and (B) symmetric nucleosome breathing. Schematic representation of discrete-state stochastic models for target search by a pioneer TF on nucleosomal DNA with (C) asymmetric breathing and (D) symmetric breathing. The protein always starts in the bulk solution, and the search process ends when the pioneer TF (red ellipse) finds its target site (red circle) located at site m along the DNA chain.

nucleosomal DNA as a lattice of $L \equiv 15$ sites, where each DNA site corresponds to 10 bps, which is the average size of the region of specific protein−DNA interactions.[3,45] For asymmetric breathing, the system can be found in one of the three major conformations (Figure 6A). The nucleosomal DNA can be fully wrapped around the octameric histone core (orange circle in Figure 6A) to form a fully wrapped (FW) conformation. Due to asymmetric unwrapping, a part of the DNA chain can dissociate from the histone surface in either the left or right end directions, forming two different partially unwrapped (PU) nucleosome conformations. For symmetric breathing, the DNA segment can independently detach simultaneously from both ends of the nucleosome, as shown in Figure 6B. The transition rates for asymmetric unwrapping/wrapping are given by k^A_{open} and k^A_{close}, respectively. Similarly, the unwrapping/wrapping transition rates for symmetric breathing are equal to k^S_{open} and k^S_{close}, respectively. Recent experiments have quantitatively measured the unwrapping rates for both asymmetric and symmetric breathing modes,[37] and similar values have been reported for these rates, allowing us to assume $k^A_{open} = k^S_{open}$. Also, it should be noted that although there are several partially unwrapped conformations as was observed in experiments,[52] to simplify our analysis it is assumed that there is only a single PU conformation for both modes of nucleosome breathing.

To quantify the protein target search, we build two discrete-state stochastic models for asymmetric and symmetric breathing modes as illustrated in Figure 6C and 6D.[23] It is assumed that the protein molecule initially starts from the solution phase (referred to as state 0) and its target site is located at site m $(1 \le m \le L)$ along the DNA chain. From the solution, the association rate to DNA depends on whether the DNA segment is naked or nucleosome-covered. The binding rate to the liberated DNA segment is k_{on} per unit site, while the corresponding binding rate to the nucleosome-covered DNA segment is equal to k'_{on}. Similarly, the dissociation rate from the free DNA is equal to k_{off}, while the rate from the nucleosome-covered region is k'_{off}. When the protein molecule is nonspecifically bound to the nucleosome-free region, it can diffuse along the DNA chain with a sliding rate u. Also, the sliding rate along the nucleosome-covered DNA segment is equal to u': see Figure 6C and 6D. The system fluctuates between FW and PU conformations with transition rates k^A_{open} and k^A_{close} for the asymmetric breathing (Figure 6C) and with rates k^S_{open} and k^S_{close} for the symmetric breathing (Figure 6D). The search process ends when the protein molecule reaches the target site located at site m $(1 \le m \le L)$ for the first time in any of the nucleosome conformations.

The transition rates for DNA unwrapping and wrapping in asymmetric breathing have already been measured,[12,15] and the corresponding values, $k^A_{open} = 210\ s^{-1}$ and $k^A_{close} = 370\ s^{-1}$, are used in our calculations. In the asymmetric breathing, we choose the length of the unwrapped DNA segment to be $l = 6$, while the number of covered DNA sites (Δ) is taken as $\Delta = 9$ (see Figure 6C). As we checked, the specific choice of the length of liberated segment l does not affect our main conclusions. In order to compare the results for asymmetric breathing with that of symmetric breathing, we choose the length of the covered DNA segment to be $\Delta = 9$ for the model presented in Figure 6D, and it automatically sets the actual lengths of the DNA segments that unwrap simultaneously from both ends as equal to $l = 3$. Furthermore, the basic assumption of our theoretical method is that pioneer TFs interact differently with the naked DNA and nucleosome-covered DNA sites.[23,27,28] Different transition rates on liberated and covered DNA segments for pioneer TFs that were utilized in our calculations are presented in Table 1.

https://doi.org/10.1021/acs.jpclett.3c03339
J. Phys. Chem. Lett. 2024, 15, 422−431

Table 1. Transition Rates for Pioneer TFs Adopted from Various Experimental Measurements[53−55]

	u (s^{-1})	u' (s^{-1})	k_{on} (s^{-1})	k'_{on} (s^{-1})	k_{off} (s^{-1})	k'_{off} (s^{-1})
Pioneer TFs	1	10	10^{-2}	10^{-4}	1	10^{-2}

To explicitly analyze the dynamics of the target search process by pioneer TFs for asymmetric and symmetric DNA unwrapping, we again explore a method of first-passage probabilities. Our idea here is to calculate the mean search times for two different modes of nucleosome breathing. For the symmetric breathing model, a full analytical solution for all dynamic properties can be obtained, as explained in the Supporting Information. For the asymmetric breathing model, Monte Carlo computer simulations are utilized.

The results of our explicit calculations of the mean search times at different target locations along the nucleosome with transition rates obtained from experiments are presented in Figure 7A. Here, we choose the number of nucleosome-covered DNA sites to be $\Delta = 9$ and compare the mean search times of pioneer TFs for only asymmetric (red curve) or only symmetric (blue curve) nucleosome breathing. One can see that for all target locations the mean search times for pioneer TFs are always faster when the nucleosome exhibits asymmetric breathing in comparison to symmetric breathing. A similar analysis for different Δ values is shown in Supporting Information Figure S6, and in all cases, the same trends are observed.

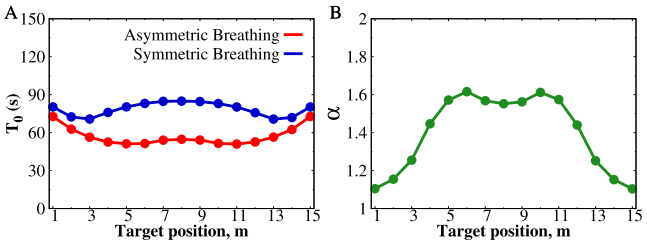

Figure 7. (A) Mean search times for pioneer TFs as a function of the target position along the DNA chain for asymmetric (red) and symmetric (blue) breathing. The solid line in symmetric breathing is obtained from analytical calculations, and symbols are from Monte Carlo computer simulations. The error bars for each symbol are defined as the standard errors, and the associated error bars are smaller than the symbol size. We also calculated the coefficient of variation of the search times, and the corresponding result is shown in Supporting Information Figure S5. (B) Acceleration in the search times for asymmetric breathing in comparison to symmetric breathing as a function of the target position. The following parameters are used in calculations: $L = 15$, $l = 6$ (for asymmetric breathing), $l = 3$ (for symmetric breathing), $\Delta = 9$, $k^A_{open} = k^S_{open} = 210\ s^{-1}$, and $k^A_{close} = k^S_{close} = 370\ s^{-1}$. All other transition rates for pioneer TF are adopted from Table 1.

To quantify the speed of the search when nucleosome breathing is asymmetric, we define a dimensionless parameter α

$$\alpha = \frac{T_0(\text{symmetric breathing})}{T_0(\text{asymmetric breathing})} \tag{10}$$

It is just a ratio of the mean search times to find their specific target for the symmetric and asymmetric modes of DNA unwrapping. When $\alpha < 1$, the search is faster for the symmetric unwrapping, while $\alpha > 1$ corresponds to the asymmetric pathway supporting the fastest target search. Figure 7B exhibits the results of our theoretical calculations that utilize experimentally measured transition rates. As one can see, pioneer TFs can find the targets that are located in the center of the system ($\alpha \approx 1.6$) faster, while the search acceleration is weaker for the target sites at the ends of the lattice. This can be explained by the observation that the DNA sites in the middle of the lattice are nucleosome-covered. As shown by recent experiments,[53,56] pioneer TFs can stay longer on such sites, allowing them to find their targets faster. It is important to note that our theoretical predictions for the search times for hidden DNA sites are in agreement with the recent *in vivo* experiments for the GAGA pioneer TFs in live Drosophila hemocytes,[57] giving additional support to our theoretical arguments. More specifically, our predictions for mean search times for pioneer TFs (Figure 7A) agree with experimentally measured search times of ∼100 s. Thus, we might conclude that nature indeed could optimize pioneer TFs to take advantage of the symmetry of nucleosome breathing. Pioneer TFs are able to enter chromatic structures faster due to asymmetric DNA unwrapping from the nucleosome particle.

In this study, we developed a theoretical approach that allowed us to explain the experimentally observed preference for asymmetric nucleosome breathing. By mapping the DNA wrapping/unwrapping processes into a set of stochastic transitions, we are able to account for all possible discrete chemical states in the system. Then the analysis of different pathways starting from the fully wrapped state and ending at the fully unwrapped state using first-passage probabilities and Monte Carlo computer simulations provided us with a comprehensive description of the nucleosome breathing dynamics processes. Explicit calculations suggest that nucleosomes prefer to unwrap asymmetrically from either end, and the probability of the pathways for strictly asymmetric unwrapping/wrapping is 2−4 orders of magnitude higher compared to that for strictly symmetric unwrapping pathways. Considering all nucleosome breathing pathways, it is still shown that asymmetric outcomes are more preferred. In addition, similar times for nucleosome eviction are predicted for all possible pathways. Furthermore, by considering an effective free-energy landscape of nucleosome breathing, we are able to give more microscopic explanations of unexpected symmetry breaking. It turns out that states along the asymmetric pathways have lower effective free energies in comparison with those of other pathways, ensuring that the system preferentially moves along these routes.

It is essential to notice that the question of why a nucleosome unwraps asymmetrically has been discussed before.[35,41] It was argued that this asymmetry is a sequence-dependent effect related to differences in DNA mechanics, and it might be specific only for the so-called Widom 601 positioning sequence that exhibits strong binding to DNA. Our theoretical approach suggests that the preference for asymmetric nucleosome unwrapping is probably a general phenomenon that should be independent of DNA sequences. Of course, the DNA sequence affects the dynamics of nucleosome breathing, but the general trend of choosing mostly the asymmetric mode is expected to be independent of this. Indeed, symmetry breaking was also observed for 5S-DNA sequences.[36,37] It will be important to experimentally study different nucleosome sequences to check the universality of asymmetric breathing.

https://doi.org/10.1021/acs.jpclett.3c03339
J. Phys. Chem. Lett. 2024, 15, 422−431

It is also important to discuss the question of equilibrium in the nucleosome breathing processes. If one considers all partially unwrapped microstates with the same degree of unwrapping (corresponding to the specific diagonal in Figure 2) as one state, then the system can be viewed as in equilibrium between fully wrapped and partially unwrapped states. However, considering different unwrapped microstates as independent states corresponds to a nonequilibrium situation, although local equilibrium can be reached for some transitions, particularly when specific conditions favor the convergence of certain microstates. In these instances, the system exhibits a transient stability, allowing for localized equilibration during the transition between the fully wrapped and partially unwrapped states. The fact that nucleosome breathing prefers asymmetric pathways is a clear sign that the system is out of equilibrium, from this point of view. This justifies our use of kinetic analysis to explain the preference for specific dynamic pathways.

Stimulated by the fact that symmetry breaking in DNA unfolding from the nucleosome's breathing might be a general phenomenon, we proposed that this is something that nature might take advantage of. To test this hypothesis, we investigated the search dynamics of pioneer TFs for specific targets on DNA for systems that experience only asymmetric breathing and only symmetric breathing. The corresponding discrete-state stochastic models have been developed, allowing us to explicitly analyze the mean search times for different modes of nucleosome breathing. Our analysis clearly showed that pioneer TFs search faster if DNA unwrapping follows the asymmetric pathway, supporting our proposal. However, the accelerations estimated using experimental values of transition rates are not too large (~60% increase). At the same time, previous theoretical studies of the pioneer TFs' target search indicated that they are also optimized much more strongly for other features of nucleosome breathing.[23,27] Importantly, our theoretical calculations of the mean search times for pioneer TFs are in agreement with the corresponding live-cell experimental observations, and they are also fully supported by Monte Carlo computer simulations.

Although the presented theoretical investigation provides a plausible microscopic picture to explain the effect of symmetry in nucleosome breathing and how it might accelerate the protein target search for hidden DNA sites, it is essential to discuss its limitations. In our nucleosome eviction model, it was assumed that the free-energy cost associated with detaching a single DNA site is the same along the nucleosome, but experiments suggest a possible nonuniform dependence on the unwrapping free-energy landscape.[50,52] It might be the result of conformational changes in the histone proteins after the initial detachment of several DNA segments. It is possible to generalize our theoretical method to take this effect into account, but qualitatively, one expects that it can lead only to even stronger symmetry breaking than predicted in the current version of our model. At the same time, using computer simulations, we already considered a model of nucleosome breathing with random energies as a way to mimic DNA sequence heterogeneity, and no significant changes have been found in comparison with the uniform energies model. We also assumed a single partially unwrapped conformation for protein search dynamics, but in reality, there is an ensemble of such conformations for a given end-to-end distance.[52] Theoretical analysis can be extended to account for those states, but it is also unlikely to change our main predictions. In addition, recent experiments highlighted the importance of the nucleosome unwrapping free-energy landscape for TF occupancy and dynamics,[25] while in our method the simplest free-energy landscape is assumed. Our theoretical analysis also did not include any active ATP-dependent driving forces that might significantly affect the processes of nucleosome unwrapping. Despite these limitations, our theoretical approach still provides a clear physical−chemical picture of complex biological processes, which, importantly, can be quantitatively tested using advanced experimental and theoretical techniques.

■ ASSOCIATED CONTENT

Supporting Information

The Supporting Information is available free of charge at https://pubs.acs.org/doi/10.1021/acs.jpclett.3c03339.

Details of analytical calculations for mean first-passage times of nucleosome eviction through asymmetric and symmetric breathing, derivation of the mean search times to locate the target site by pioneer TFs in the presence of symmetric nucleosome breathing dynamics, and Monte Carlo simulation details (PDF)

■ AUTHOR INFORMATION

Corresponding Author

Anatoly B. Kolomeisky − *Center for Theoretical Biological Physics, Department of Chemistry, and Department of Chemical and Biomolecular Engineering, Rice University, Houston, Texas 77005, United States;* orcid.org/0000-0001-5677-6690; Email: tolya@rice.edu

Author

Anupam Mondal − *Center for Theoretical Biological Physics and Department of Chemistry, Rice University, Houston, Texas 77005, United States;* orcid.org/0000-0002-8436-5618

Complete contact information is available at: https://pubs.acs.org/10.1021/acs.jpclett.3c03339

Notes

The authors declare no competing financial interest.

■ ACKNOWLEDGMENTS

The work was supported by the Welch Foundation (C-1559), by the NSF (CHE-2246878), and by the Center for Theoretical Biological Physics sponsored by the NSF (PHY-2019745).

■ REFERENCES

(1) Lodish, H.; Berk, A.; Kaiser, C. A.; Krieger, M.; Scott, M. P.; Bretscher, A.; Ploegh, H.; Matsudaira, P. *Molecular Cell Biology*; Macmillan: New York, 2008.

(2) Phillips, R.; Kondev, J.; Theriot, J.; Garcia, H. G.; Orme, N. *Physical Biology of the Cell*; Garland Science: New York, 2012.

(3) Shvets, A. A.; Kochugaeva, M. P.; Kolomeisky, A. B. Mechanisms of protein search for targets on DNA: theoretical insights. *Molecules* **2018**, *23*, 2106.

(4) Iwahara, J.; Kolomeisky, A. B. Discrete-state stochastic kinetic models for target DNA search by proteins: Theory and experimental applications. *Biophys Chem.* **2021**, *269*, No. 106521.

(5) Luger, K.; Mader, A. W.; Richmond, R. K.; Sargent, D. F.; Richmond, T. J. Crystal structure of the nucleosome core particle at 2.8 Å resolution. *Nature* **1997**, *389*, 251−260.

(6) Richmond, T. J.; Davey, C. A. The structure of DNA in the nucleosome core. *Nature* **2003**, *423*, 145−150.
(7) Harbison, C. T.; et al. Transcriptional regulatory code of a eukaryotic genome. *Nature* **2004**, *431*, 99−104.
(8) Liu, X.; Lee, C. K.; Granek, J. A.; Clarke, N. D.; Lieb, J. D. Whole-genome comparison of Leu3 binding in vitro and in vivo reveals the importance of nucleosome occupancy in target site selection. *Genome Res.* **2006**, *16*, 1517−1528.
(9) Pique-Regi, R.; Degner, J. F.; Pai, A. A.; Gaffney, D. J.; Gilad, Y.; Pritchard, J. K. Accurate inference of transcription factor binding from DNA sequence and chromatin accessibility data. *Genome Res.* **2011**, *21*, 447−455.
(10) Polach, K. J.; Widom, J. Mechanism of protein access to specific DNA sequences in chromatin: a dynamic equilibrium model for gene regulation. *J. Mol. Biol.* **1995**, *254*, 130−149.
(11) Li, G.; Widom, J. Nucleosomes facilitate their own invasion. *Nat. Struct Mol. Biol.* **2004**, *11*, 763−769.
(12) Li, G.; Levitus, M.; Bustamante, C.; Widom, J. Rapid spontaneous accessibility of nucleosomal DNA. *Nat. Struct Mol. Biol.* **2005**, *12*, 46−53.
(13) Tims, H. S.; Gurunathan, K.; Levitus, M.; Widom, J. Dynamics of nucleosome invasion by DNA binding proteins. *J. Mol. Biol.* **2011**, *411*, 430−448.
(14) Winogradoff, D.; Aksimentiev, A. Molecular mechanism of spontaneous nucleosome unraveling. *J. Mol. Biol.* **2019**, *431*, 323−335.
(15) Kim, J.; Lee, J.; Lee, T. H. Lysine acetylation facilitates spontaneous DNA dynamics in the nucleosome. *J. Phys. Chem. B* **2015**, *119*, 15001−15005.
(16) Iwafuchi-Doi, M.; Zaret, K. S. Cell fate control by pioneer transcription factors. *Development* **2016**, *143*, 1833−1837.
(17) Iwafuchi-Doi, M.; Zaret, K. S. Pioneer transcription factors in cell reprogramming. *Genes Dev.* **2014**, *28*, 2679−2692.
(18) Zaret, K. S.; Mango, S. E. Pioneer transcription factors, chromatin dynamics, and cell fate control. *Curr. Opin Genet Dev* **2016**, *37*, 76−81.
(19) Zaret, K. S.; Carroll, J. S. Pioneer transcription factors: establishing competence for gene expression. *Genes Dev.* **2011**, *25*, 2227−2241.
(20) Slattery, M.; Zhou, T.; Yang, L.; Dantas Machado, A. C.; Gordan, R.; Rohs, R. Absence of a simple code: how transcription factors read the genome. *Trends Biochem. Sci.* **2014**, *39*, 381−399.
(21) Cirillo, L. A.; Lin, F. R.; Cuesta, I.; Friedman, D.; Jarnik, M.; Zaret, K. S. Opening of compacted chromatin by early developmental transcription factors HNF3 (FoxA) and GATA-4. *Mol. Cell* **2002**, *9*, 279−289.
(22) Jozwik, K. M.; Carroll, J. S. Pioneer factors in hormone-dependent cancers. *Nat. Rev. Cancer* **2012**, *12*, 381−385.
(23) Mondal, A.; Felipe, C.; Kolomeisky, A. B. Nucleosome breathing facilitates the search for hidden DNA sites by pioneer transcription factors. *J. Phys. Chem. Lett.* **2023**, *14*, 4096−4103.
(24) Schiessel, H. Telling left from right in breathing nucleosomes. *Biophys. J.* **2018**, *115*, 749−750.
(25) Donovan, B. T.; Luo, Y.; Meng, Z.; Poirier, M. G. The nucleosome unwrapping free energy landscape defines distinct regions of transcription factor accessibility and kinetics. *Nucleic Acids Res.* **2023**, *51*, 1139−1153.
(26) Mondal, A.; Mishra, S. K.; Bhattacherjee, A. Kinetic origin of nucleosome invasion by pioneer transcription factors. *Biophys. J.* **2021**, *120*, 5219−5230.
(27) Felipe, C.; Shin, J.; Kolomeisky, A. B. How pioneer transcription factors search for target sites on nucleosomal DNA. *J. Phys. Chem. B* **2022**, *126*, 4061−4068.
(28) Mondal, A.; Kolomeisky, A. B. Role of nucleosome sliding in the protein target search for covered DNA sites. *J. Phys. Chem. Lett.* **2023**, *14*, 7073−7082.
(29) Mishra, S. K.; Bhattacherjee, A. How do nucleosome dynamics regulate protein search on DNA? *J. Phys. Chem. B* **2023**, *127*, 5702−5717.
(30) Li, X.; Chou, T. Stochastic nucleosome disassembly mediated by remodelers and histone fragmentation. *J. Chem. Phys.* **2023**, *159*, No. 204107.
(31) Kelbauskas, L.; Woodbury, N.; Lohr, D. DNA sequence-dependent variation in nucleosome structure, stability, and dynamics detected by a FRET-based analysis. *Biochem Cell Biol.* **2009**, *87*, 323−335.
(32) Koopmans, W. J.; Buning, R.; Schmidt, T.; van Noort, J. spFRET using alternating excitation and FCS reveals progressive DNA unwrapping in nucleosomes. *Biophys. J.* **2009**, *97*, 195−204.
(33) North, J. A.; Shimko, J. C.; Javaid, S.; Mooney, A. M.; Shoffner, M. A.; Rose, S. D.; Bundschuh, R.; Fishel, R.; Ottesen, J. J.; Poirier, M. G. Regulation of the nucleosome unwrapping rate controls DNA accessibility. *Nucleic Acids Res.* **2012**, *40*, 10215−10227.
(34) Andresen, K.; Jimenez-Useche, I.; Howell, S. C.; Yuan, C.; Qiu, X. Solution scattering and FRET studies on nucleosomes reveal DNA unwrapping effects of H3 and H4 tail removal. *PLoS One* **2013**, *8*, No. e78587.
(35) Ngo, T. T.; Zhang, Q.; Zhou, R.; Yodh, J. G.; Ha, T. Asymmetric unwrapping of nucleosomes under tension directed by DNA local flexibility. *Cell* **2015**, *160*, 1135−1144.
(36) Chen, Y.; Tokuda, J. M.; Topping, T.; Sutton, J. L.; Meisburger, S. P.; Pabit, S. A.; Gloss, L. M.; Pollack, L. Revealing transient structures of nucleosomes as DNA unwinds. *Nucleic Acids Res.* **2014**, *42*, 8767−8776.
(37) Chen, Y.; Tokuda, J. M.; Topping, T.; Meisburger, S. P.; Pabit, S. A.; Gloss, L. M.; Pollack, L. Asymmetric unwrapping of nucleosomal DNA propagates asymmetric opening and dissociation of the histone core. *Proc. Natl. Acad. Sci. U. S. A.* **2017**, *114*, 334−339.
(38) Mauney, A. W.; Tokuda, J. M.; Gloss, L. M.; Gonzalez, O.; Pollack, L. Local DNA sequence controls asymmetry of DNA unwrapping from nucleosome core particles. *Biophys. J.* **2018**, *115*, 773−781.
(39) Bilokapic, S.; Strauss, M.; Halic, M. Histone octamer rearranges to adapt to DNA unwrapping. *Nat. Struct Mol. Biol.* **2018**, *25*, 101−108.
(40) Konrad, S. F.; Vanderlinden, W.; Frederickx, W.; Brouns, T.; Menze, B. H.; De Feyter, S.; Lipfert, J. High-throughput AFM analysis reveals unwrapping pathways of H3 and CENP-A nucleosomes. *Nanoscale* **2021**, *13*, 5435−5447.
(41) de Bruin, L.; Tompitak, M.; Eslami-Mossallam, B.; Schiessel, H. Why do nucleosomes unwrap asymmetrically? *J. Phys. Chem. B* **2016**, *120*, 5855−5863.
(42) Zhang, B.; Zheng, W.; Papoian, G. A.; Wolynes, P. G. Exploring the free energy landscape of nucleosomes. *J. Am. Chem. Soc.* **2016**, *138*, 8126−8133.
(43) Armeev, G. A.; Kniazeva, A. S.; Komarova, G. A.; Kirpichnikov, M. P.; Shaytan, A. K. Histone dynamics mediate DNA unwrapping and sliding in nucleosomes. *Nat. Commun.* **2021**, *12*, 2387.
(44) Mondal, A.; Mishra, S. K.; Bhattacherjee, A. Nucleosome breathing facilitates cooperative binding of pluripotency factors Sox2 and Oct4 to DNA. *Biophys. J.* **2022**, *121*, 4526−4542.
(45) Felipe, C.; Shin, J.; Loginova, Y.; Kolomeisky, A. B. The effect of obstacles in multi-site protein target search with DNA looping. *J. Chem. Phys.* **2020**, *152*, No. 025101.
(46) Shvets, A. A.; Kolomeisky, A. B. The role of DNA looping in the search for specific targets on DNA by multisite proteins. *J. Phys. Chem. Lett.* **2016**, *7*, 5022−5027.
(47) Shvets, A. A.; Kolomeisky, A. B. Sequence heterogeneity accelerates protein search for targets on DNA. *J. Chem. Phys.* **2015**, *143*, No. 245101.
(48) Kolomeisky, A. B. *Motor Proteins and Molecular Motors*; CRC Press, Boca Raton, FL, 2015.
(49) Li, X.; Kolomeisky, A. B. Mechanisms and topology determination of complex chemical and biological network systems from first-passage theoretical approach. *J. Chem. Phys.* **2013**, *139*, No. 144106.

https://doi.org/10.1021/acs.jpclett.3c03339
J. Phys. Chem. Lett. 2024, 15, 422−431

(50) Forties, R. A.; North, J. A.; Javaid, S.; Tabbaa, O. P.; Fishel, R.; Poirier, M. G.; Bundschuh, R. A quantitative model of nucleosome dynamics. *Nucleic Acids Res.* **2011**, *39*, 8306−8313.
(51) Teimouri, H.; Spaulding, C.; Kolomeisky, A. B. Optimal pathways control fixation of multiple mutations during cancer initiation. *Biophys. J.* **2022**, *121*, 3698−3705.
(52) Zhao, D.; Le, J. V.; Darcy, M. A.; Crocker, K.; Poirier, M. G.; Castro, C.; Bundschuh, R. Quantitative modeling of nucleosome unwrapping from both ends. *Biophys. J.* **2019**, *117*, 2204−2216.
(53) Donovan, B. T.; Chen, H.; Jipa, C.; Bai, L.; Poirier, M. G. Dissociation rate compensation mechanism for budding yeast pioneer transcription factors. *Elife* **2019**, *8*, DOI: 10.7554/eLife.43008.
(54) Luo, Y.; North, J. A.; Rose, S. D.; Poirier, M. G. Nucleosomes accelerate transcription factor dissociation. *Nucleic Acids Res.* **2014**, *42*, 3017−3027.
(55) Luo, Y.; North, J. A.; Poirier, M. G. Single molecule fluorescence methodologies for investigating transcription factor binding kinetics to nucleosomes and DNA. *Methods* **2014**, *70*, 108−118.
(56) Donovan, B. T.; Chen, H.; Eek, P.; Meng, Z.; Jipa, C.; Tan, S.; Bai, L.; Poirier, M. G. Basic helix-loop-helix pioneer factors interact with the histone octamer to invade nucleosomes and generate nucleosome-depleted regions. *Mol. Cell* **2023**, *83*, 1251−1263.
(57) Tang, X.; Li, T.; Liu, S.; Wisniewski, J.; Zheng, Q.; Rong, Y.; Lavis, L. D.; Wu, C. Kinetic principles underlying pioneer function of GAGA transcription factor in live cells. *Nat. Struct Mol. Biol.* **2022**, *29*, 665−676.

https://doi.org/10.1021/acs.jpclett.3c03339
J. Phys. Chem. Lett. 2024, 15, 422−431